

## Introduction: Hydraulic Effects in the Ocean and Atmosphere

‘Hydraulics’ is a nebulous term that evokes images of pumps, dams, brake fluid and lifting machines. In geophysics the term has been applied to wind or current systems that exhibit behavior found in spillways, aqueducts, dams and other open channel engineering applications. Many oceanic and atmospheric flows are topographically constrained in the same way that rivers and reservoirs are, and so it is not surprising that similar physical features arise. For instance, the spillage of dense air over a mountain range and the resultant strong down-slope winds are visually and dynamically similar to the flow of water over a dam or weir. Overflows of dense water flowing along the ocean bottom or in sea straits exhibit similar behavior. The term *rotating hydraulics* has been used to describe the peculiar physical features that arise when hydraulic behavior occurs in flows sufficiently broad to be influenced by the earth’s rotation. Examples may include large-scale oceanic flows such as jets and coastal currents that bear little resemblance to open-channel flows. Precisely what do geophysicists mean when they talk about hydraulics and why should one listen?

A good starting point in the understanding of hydraulic phenomena is the principle of signal or information propagation along a conduit. There are a variety of ways that fluids can transmit information, including advection by a velocity field and wave propagation. Most of what we think of as hydraulic behavior is manifested by signal propagation due to waves. As an example, consider the steady flow of water over a dam (Figure I1). The flow originates from a deep reservoir and spills across the crest or sill of the dam and down the spillway. At the base of the spillway is a hydraulic jump, an abrupt increase in the fluid depth accompanied by intense turbulence. Although the flow is steady, we can imagine the effect of temporarily disturbing the fluid at some location in order to observe where the resulting waves travel. The travel paths tell us something about how information propagates through the system. If the flow is disturbed upstream of the dam crest, the waves that are generated can propagate in either direction, as suggested by the wavy arrows in the Figure. We call this type of flow *subcritical*. On the other hand, the flow immediately downstream of the crest is so rapid that waves are prevented from propagating in the upstream direction. We call this flow *supercritical*. As the fluid passes through the hydraulic jump, it is returned to a subcritical state. At the crest of the dam the flow is *critical*, meaning that the wave that would otherwise propagate towards the reservoir is frozen. Clearly, the reservoir flow cannot be affected by a change in conditions downstream of the dam crest; the information generated would never reach the reservoir. On the other hand, the reservoir *is* influenced by the characteristics of the dam itself. In fact, we would say that the dam *is* the downstream source of information. The outflow from the reservoir is said to be *choked* or *hydraulically controlled* by the dam. The exact meaning of these terms will be discussed at length in Chapter 1, but for now we simply think of ‘control’ as the ability of the dam to regulate the volume flow rate and the reservoir level.

As an example of flow regulation, suppose that the reservoir is fed by river runoff and drained at the same rate by the discharge over the dam. The whole system is in a steady state. If the elevation of the dam crest is then raised, the height of the reservoir surface above the dam is diminished and the volume outflow decreases. The river runoff now exceeds the outflow and the excess is stored in the reservoir. The reservoir level rises and eventually the original outflow rate is restored. The actual sequence of events may be a little more complicated than what we have described, but the result is essentially correct: the dam influences the time history of the discharge.

There are many fluid systems that experience choking or regulation in an analogous manner. One is the transonic flow of a compressible gas in a wind tunnel. The flow is subsonic in the wider, upstream section of the tunnel, meaning that sound waves can propagate upstream and downstream. The tunnel narrows to its most constricted area at midsection and there a transition to supersonic flow occurs. The tunnel widens farther downstream but the flow remains supersonic. There, sound wave propagation can occur only in the downstream direction.

*a. The defining characteristics of hydraulic behavior in geophysics.*

We can now identify two conditions that typify hydraulic behavior and serve as criteria for the examples included in this book. The first is that large variations in the flow properties occur along the predominant flow direction. In the example sketched in Figure I1, large variations in fluid depth and velocity occur as the fluid passes over the dam and moves from a subcritical to a supercritical state. Large variations also occur where the flow passes through the hydraulic jump. ‘Large’ generally means that the along-stream variations in the depth and velocity are as large as the mean values of these quantities. There are some exceptions in which traditional features such as subcritical-to-supercritical transitions occur without dramatic changes in structure.

The second (and most important) characteristic feature of hydraulic behavior is that the flow in question develops velocities large enough to arrest the propagation of information by waves. If  $c$  represents the linear phase speed of a particular wave, then blockage of information apparently means that  $c$  goes to zero somewhere in the fluid domain. In many cases,  $c$  is composed of the sum of an advection speed  $U$ , where  $U$  is a characteristic fluid velocity scale, and a relative (or ‘intrinsic’) wave speed  $c'$ . Thus  $c \equiv U + c'$  and  $c=0$  requires  $U / c' = 1$ .

If no restriction is put on the type or scale of wave under consideration, the condition  $U / c' \cong 1$  can readily occur. For example, the speed of a free surface gravity wave of length  $\lambda$ , propagating in a homogeneous stream of uniform depth  $D$  and velocity  $U$ , is given by

$$c = U \pm \left( \frac{g\lambda}{2\pi} \tanh\left(\frac{2\pi D}{\lambda}\right) \right)^{1/2},$$

where  $g$  is the gravitational acceleration. The intrinsic wave speed, the second term on the right-hand side, varies from zero to  $\pm(gD)^{1/2}$  as  $\lambda/D$  ranges from zero to infinity. Thus it is possible for all  $U < (gD)^{1/2}$  to find a wave length such that  $c=0$ . In fact the true situation is more complicated; for reasons to be explained in later chapters, dispersive waves, ones having  $dc/d\lambda \neq 0$ , are inconsequential to hydraulic behavior. Only the nondispersive waves ( $dc/d\lambda = 0$ ) carry information that can efficiently alter the flow on which they propagate. In the present example, nondispersive behavior occurs in the long-wave limit ( $\lambda/D \gg 1$ ), with  $c \rightarrow U \pm (gD)^{1/2}$ . Thus hydraulic behavior occurs when  $U$  is as large as  $(gD)^{1/2}$ . In the majority of cases, hydraulic behavior is dominated by long wave dynamics, and  $c'$  in the criterion  $U/c' \cong 1$  pertains only to such waves. With this view, the condition  $U/c' \cong O(1)$  becomes much more restrictive.

If several classes of waves exist, then hydraulic behavior with respect to a certain class is possible if  $U/c' \cong 1$  for the nondispersive waves in that class. If the typical  $c$  values are much less, or much greater than  $U$ , for other classes, then hydraulic effects are not expected with respect to these classes. In the example of the overflow shown in Figure I1, the fluid can support both sound waves and free surface gravity waves. However, the former travel much faster than the typical fluid speeds and are inconsequential to hydraulic behavior. In ocean straits, where the depth  $D$  can range from several hundred to several thousand meters, the value of  $(gD)^{1/2}$  exceeds 50m/s, which is far greater than the typical velocities (<2m/s). So free-surface, long gravity waves in the ocean are largely irrelevant for hydraulic behavior in major straits. However, the ocean and atmosphere are density stratified as the result of variations in temperature, salinity and/or humidity. Stratification gives rise to the presence of *internal* gravity waves, in which gravity remains the restoring force but where the effective value of  $g$  is reduced in proportion to the vertical density (or potential density) gradient. The corresponding long wave speeds lies in the range of the fluid velocities observed in the ocean and atmosphere and hydraulic effects are therefore possible. Such behavior is sometimes referred to as *internal hydraulics*.

In summary, hydraulic effects arise in flows that are rapid enough to arrest nondispersive waves and that undergo large transitions of velocity and layer depth along the predominant direction of the current. An important consequence of these properties is nonlinearity. Processes such as hydraulic control and features like jumps and bores are fundamentally nonlinear. Nonlinearity gives rise to multiple solutions and part of the challenge is to identify the solutions that are physically robust. Nonlinearity also forces one to stretch his or her intuition and, in some cases, take a leap beyond traditional linear thinking. This is what makes the study of hydraulic phenomena fun.

#### *b. Examples of hydraulic phenomena in geophysics.*

The atmosphere exhibits hydraulic behavior, the most familiar examples being the severe downslope winds generated when dense air masses spill over mountain ranges. The Chinook winds of the American Rocky Mountains, the Santa Annas of southern California, and the Mistral of Provence, and the Boras of the Adriatic Sea are all well

documented. Rotational effects in such cases tend to be limited by the relatively small spatial extent of the spilling flows. A case in which rotation is more important involves the winds in the California coastal marine layer, a relatively dense and well-mixed slab of moist air that occupies the lower 300-600m of the atmosphere above the sea surface in that region. The interface that separates the moist air from the overlying lighter and drier air can be quite sharp. The marine layer itself can be seen in images of low-level cloud cover (Figure I2a). Mountain ranges along the California coast steer the marine layer winds along to the coast, here towards the southeast direction. Point Arena and other promontories constrict or choke the winds, causing them to accelerate and become supercritical with respect to an internal Kelvin wave. The latter is an internal gravity wave that propagates on the upper boundary of the marine layer and is trapped to the coast. The supercritical flow is marked by an area of clear air to the southeast of Point Arena. The clear area terminates abruptly near Bodega Bay in a cloudy region that contains streaks or undulations that sweep far offshore. The leading edge of this feature is thought to be a type of hydraulic jump. The velocity arrows and isopleths for a similar event are shown in Figure I2b. In this case the hydraulic jump occurs at Stewarts Point. In contrast to the picture of nonrotating hydraulic control (Figure 1), the choking effect in these examples is due to the protrusion of a single sidewall into the path of the current.

When the prevailing northwesterly winds relax, the marine layer may reverse direction and flow towards the northwest (Figure I2c). The intrusion of cloudy moist air that moves along the coast resembles a *gravity current*, a flow created in a rotating environment when dense fluid is allowed to spill into a less dense environment. If a wall is present, the gravitationally driven current will remain trapped to it. For the case shown in Figure I2c, the moist air of the marine layer plays the role of the dense flow. Gravity currents and other coastal flows will be discussed further in Chapter 4.

Many examples of rotationally influenced hydraulic phenomena arise within the abyssal, basin-to-basin flow in the oceans. This circulation is sometimes thought of as the lower limbs of a great 'conveyor belt', a schematic representation of broad transports at different levels between the major oceans (Figure I3). Changes in the strength or direction of the overturning cells within this scheme have been linked to rapid climate change. A resident of Northern Europe might begin her description of the conveyor in the North Atlantic area with a (white) northward surface current consisting of the Gulf Stream and its extension, the North Atlantic Current. These currents transport relatively warm, saline water into the Nordic Seas north of Iceland and Scotland. There, concentrated distillation, cooling, freezing and mixing at the sea surface cause some of the surface water to become unstably stratified and to overturn, sometimes resulting in sinking to great depth. The geographic distribution of mixing and deep sinking is not completely understood, but it is known that the resulting deep-water masses move away from their convective origin. They spill out of the Nordic Seas and flow equatorward in a deep western boundary current (colored grey in Figure I3). Before it reaches the equator, this *North Atlantic Deep Water* (hereafter NADW) detaches from the bottom, riding up over a water mass of Antarctic origin (black path). Some portion of NADW continues southward, enters the Antarctic Circumpolar Current, and eventually makes its way into the Indian and Pacific Oceans. It gradually wells up and becomes part of the

(white) warmer and fresher surface currents that transport water from the Pacific to the Indian Ocean and eventually back into the Atlantic, to complete the meridional overturning cell.

The second main contributor to the abyssal circulation is the aforementioned *Antarctic Bottom Water* (AABW). This water mass is formed in the Weddell and Ross Seas and over the greater continental shelves of Antarctica. This water flows northward along the bottom into the Atlantic, Indian, and Pacific Oceans where it mixes and wells up. It is believed that the upward movement and mixing of AABW and NADW is enhanced over regions of rough topography.

A viewer of Figure I3 should be aware of several caveats. One is that the ocean circulation is strongly time dependent and the transport of water and other properties can be strongly affected by fluctuating eddy processes. Not all the pathways suggested should be interpreted as persistent currents, nor do they always suggest the direct paths of typical water parcels. For example, a parcel of NADW entering the Circumpolar Current from the Atlantic may spin around Antarctica multiple times before exiting into the Indian or Pacific Oceans, or it may simply re-enter the Atlantic. In addition, the figure does not acknowledge sinking regions that lie at the margins of the Atlantic and Southern Oceans and in marginal seas. For example, deep convection in the Labrador Sea is known to contribute to North Atlantic Deep Water. Dense water masses are also produced in the Red and Mediterranean Seas. The salty outflows from these seas spread and circulate in the Indian and Atlantic Oceans, respectively, in ways that are not fully understood.

Hydraulic effects occurring within the lower limbs of the conveyor are due to interactions with bottom topography. The bottom is a bumpy collection of old tectonic plates surrounded by hotspot tracks, swells, flood basalts, pieces of thickened crust, and ridges. The latter subdivide the major oceans into numerous basins (Figures I4a,b,c). The abyssal currents that form the lowest limbs of the conveyor make their way from basin to basin, seeking out the deepest connecting strait or sill. Some of these deep flows are observed to spill into the downstream basin in roughly the same manner as flow over a dam. The volume flux of the spilling flows can double or triple as the result of mixing with and entrainment of overlying water. A deep current will sometimes flow into a terminal basin; there, it mixes with overlying water and gradually rises to shallower levels.

Some of the major passages in which overflows are observed have been indicated in Figures I4a,b,c. Each example has been documented by the direct measurement of deep velocities. Also shown are the locations of several prominent straits connecting marginal seas to the ocean proper. These shallower passages generally contain exchange flows (a double arrow), often with an inflowing surface current overlying a deep outflow. Many of the passages, shallow or deep, are strategically advantageous locations for the measurement of property fluxes relevant to the ocean circulation and to global climate. They funnel massive flows through a relatively small area and they may be candidates for the same type of hydraulic monitoring that engineers use to keep track of the outflow

from a reservoir. The overflows can have distinct chemical distributions and a time-history of this chemistry can be extracted from deep sediments and used to infer properties of the thermohaline circulation through geological time.

The most thoroughly documented deep overflows are those of the North Atlantic and these are now described in more detail. The two main water masses involved, NAWD and AABW, can be identified in a north-south section of potential density ( $\sigma_4$ )<sup>1</sup> in the western Atlantic (Figure I5). The section track is shown in I6a, which also gives a plan view of the ocean bottom and the 1.8°C potential temperature<sup>2</sup> surface. The geographical distribution of this surface gives some indication of the spreading of the deep water masses away from their source. The reader should interpret both figures with caution: the thinning or dilution of a water mass in a particular direction need not indicate a flow in that direction.

AABW enters the western Atlantic across the south boundary of the Figure I5a section and generally spreads northward into the Argentine Basin. The overall northward movement is known from temperature, salinity, silicate and other properties suggesting an Antarctic origin, and from observations of northward flow in deep straits such as the Vema Channel, where spilling is also observed. After passing through the Vema and Hunter Channels, AABW enters the Brazil Basin. Along this path, the deep isopycnal surfaces deepen in a way that suggests spilling. This deepening could also be the result of mixing with overlying water or the presence of transverse (east-west) geostrophic flow. However, direct measurements show that AABW exits the basin in two directions. To the west is the Ceara Abyssal Plain that serves as a complex and very broad sill leading into the Western North Atlantic Basin. The Figure I5 transect, which crosses this plain, shows that the isopycnal surfaces with  $\sigma_4 \geq 45.9$  progressively deepen, and eventually ground, to the north and across the Western North Atlantic Basin. The second exit lies to the east and through the mid-Atlantic Ridge, which is transected by the Romanche and Chain Fracture Zones (Figure I4a). Some AABW passes across the sills of these passages and into the Eastern Atlantic, while some continues northward along the western flank of the ridge. Some of this northward flow turns east and passes through the ridge within the Vema Fracture Zone at 11° N. All of the eastward flows that cross the ridge spill and mix into the basins of the eastern Atlantic. In the case of the Vema Fracture Zone, some of the overflow water has been mixed to the point where  $\sigma_4 < 46.0$ . The diluted water makes its way to Discovery Gap at about 36° N and eventually terminates.

The deep waters entering the Atlantic from the north spill across Greenland-Iceland-Scotland ridges through two main passages: the Denmark Strait (650m sill depth) and Faroe Bank Channel (880m). The two outflows merge to form NADW, which

---

<sup>1</sup>  $\sigma_4$  is the density that a water parcel would have if that parcel were moved to a pressure of 4000 decibars (db), roughly equivalent to 4000m depth. The 4000 db reference level is used to avoid difficulties that arise in connection with nonlinearities in the equation of state. For example, use of the sea surface as a reference pressure would lead in some cases to the conclusion that the deep stratification is hydrostatically unstable.

<sup>2</sup> In all cases, potential temperature refers to the temperature a fluid parcel would have if that parcel were moved adiabatically to ocean surface pressure (zero db).

moves southward in the aforementioned deep western boundary current. Its transport is augmented by deep convection in the Labrador Sea. The overall southward flow is complicated by branching, eddying, and mixing of the boundary current. As a result, the NADW becomes spread over the bottom of the western North Atlantic basin southward until it encounters AABW and leaves the bottom, as shown in Figure I5. The presence and spreading of both NADW and AABW is also suggested by Figure I6a map of water with potential temperatures greater than 1.8°C.

The Denmark Strait provided some of the first observations of deep-ocean hydraulic behavior. The draw down of isopycnals associated with the southward spilling, apparent in Figure I5, is shown in more detail (Figure I7). Most of the mixing and entrainment that occurs in this and other major overflows takes place in a 'plume' or 'outflow' region, roughly corresponding to the descending region downstream of the sill. The transverse structure of the flow (Figure I8) is strongly influenced by the earth's rotation, which causes the isopycnals to tilt and the overflow water ( $\sigma_\theta > 27.6$ ) to bank against the Greenland continental slope. The details of this structure can be quite variable in time. The Faroe-Bank Channel overflow exhibits some of the same features and will be the subject of a more detailed examination (Section 2.11).

The overflow in the Faroe Bank Channel exhibits similar features. The deepest water in this passage is denser than that of the Denmark Strait. The overflow descends into the Iceland Basin to depths of about 3500 meters. The water then flows southward along the flanks of the mid-Atlantic Ridge until it encounters the Charlie-Gibbs fracture zone. Most of the flow continues westward through this gap, where it joins the Denmark Strait overflow. A more detailed examination of this overflow appears in Section 2.11.

Other oceanographically important, deep passages with overflows exist in the Pacific and Indian Oceans. In the Pacific, the Samoan passage (Figure I3b) has clearly defined currents that carry a mixture of North Atlantic Deep Water and Antarctic Bottom Water north. The inlet to the Panama basin near South America contains a bottom current feeding the deep basin. To the west, there are many sub-basins in the Indonesian-Philippine Basin, each with a deep inlet and an inflow of dense water. In the Indian Ocean (Figure I3c) there are overflows across the Ninety-East Ridge and in the Amirante Passage. The spreading of dense water masses in these locations is suggested in Figures I6b and I6c, which map the 1.0°C potential temperature surface.

#### *d. Exchange flows.*

To this point, we have treated overflows as unidirectional and isolated, paying little attention to interactions with the overlying fluid. Indeed, the neglect of interactions with the overlying layers is an assumption held by many models. However relevant this view may be to the deep ocean, it rarely applies in the shallow straits separating marginal seas from the major oceans. Bodies such as the Red and Mediterranean Seas act as *inverse estuaries* by losing more fresh water to evaporation than is gained by river runoff and precipitation. Salt is concentrated in the surface layers and this makes the water more susceptible to deep convection due to localized atmospheric cooling events. For

example, deep convection has been observed in the Gulf of Lyon and in the far northern reaches of the Red Sea. The dense waters accumulate and spill out through relatively shallow straits such as the Bab al Mandab and Strait of Gibraltar. Mass and salt conservation require that the dense waters be replaced and this occurs in the form of surface inflow. *Exchange flows* with opposing upper and lower layers of comparable depth and velocity are thereby set up in the connecting straits. An exchange flow also occurs in the Bosphorus, a narrow strait separating the Mediterranean and Black Seas.

One of the earliest references to exchange flows in sea straits was a set of remarks by Smith (1684) on the Strait of Gibraltar. Smith knew about the surface inflow:

“There is a vast draught of water poured continually out of the Atlantic into the Mediterranean; the mouth or entrance of which between Cape Spartel or Sprat, as the seamen call it, and Cape Trafalgar, may be near 7 leagues wide, the current setting strong into it, and not losing its force till it runs as far as Malaga, which is about 20 leagues within the Straits.”

There was, at the time, much speculation about the destination of this inflow, including:

“subterraneous vents, cavities, and indraughts, exhalations by the sun beams, the running out of the water on the African side, as if there were a kind of circular motion of the water, and that it only flowed in upon the Christian shore”.

Smith considered these conjectures fanciful and contrary to observation. His hypothesis was that the surface inflow must be balanced by a deep outflow in the Strait:

“an under-current, by which as great a quantity of water is carried out as comes flowing in”.

Smith’s theory was not based on mass conservation alone. He had heard a report from a sailor aboard a vessel that had attempted to enter the Baltic Sea through the Öresund, the strait that separates Denmark and Sweden:

“He told me that, being there in one of the king’s frigates, they went with their pinnance into the mid stream, and were carried violently by the current; that soon after they sunk a bucket with a large cannon ball, to a certain depth of water, which gave check to the boat’s motion, and sinking it still lower and lower, the boat was driven ahead to windward against the upper current: the current aloft, as he added, not being 4 or 5 fathom deep, and that the lower the bucket was let fall, they found the under current the stronger.”

The Gibraltar outflow descends the continental slope west of Portugal down to about 1000m to form a saline plume in the Atlantic known as the Mediterranean salt tongue. This water mass can be detected throughout the North Atlantic at intermediate depths. As documented by Armi and Farmer (1988), the Strait of Gibraltar acts as a choke point or hydraulic control on the inflow and outflow. Figure I9 shows a longitudinal acoustic image taken near the 250m deep Camerinal Sill at the western end of the Strait. The Atlantic Ocean is to the right and the Mediterranean Sea is to the left. The ship-mounted acoustic transponder generates sound waves that are scattered from fish, small particles, bubbles, and temperature microstructure. The wavy band that lies near the surface in the left-hand portion of the image approximates the interface between

the outflowing (left-to-right) lower layer and the incoming upper layer. Superimposed temperature profiles confirm that inferred interface level lies in the depth range of most rapid temperature change. Note the descent of interface into deeper water as the lower layer spills over the sill. Further downstream are some dark undulations that have been interpreted as an internal hydraulic jump. Although rotation is probably not important within the strait proper, the outflows in either direction become strongly influenced by rotation past the exits.

*e) Other Examples.*

The world's marginal seas and coastal areas also have an abundance of other straits and gaps that may be important regionally or globally and that are wide enough to feel the Earth's rotation. One example is the Strait of Sicily, which contains a current of relatively saline bottom water that flows from the eastern to the western Mediterranean. At a sill depth of 1600m, the Anegada-Jungfern Passage is the deepest inlet into the Caribbean basin (Figures I3a and I10). Dense inflows through this and other inlets supply all deep waters for the Caribbean, filling it from the bottom to about this sill depth. The passage actually contains two parallel channels, the Jungfern Passage and the Grappler Channel. The earth's rotation is evident in the intensification of the flow along the right-hand walls of both channels (Figure I11). The Baltic Sea, which acts as a giant estuary, is separated from the North Sea by a series of straits that carry fresh water seaward and allow an intermittent inflow.

Smaller scale estuaries and inverse estuaries may experience hydraulic effects as well. Another important body that experience estuary dynamics but is large enough to be influenced by the earth's rotation is Chesapeake Bay, North America (Figure I12a,b). Although there is no evidence for hydraulic control of the exchange flow that occurs at the mouth, the bay is the source of an important rotating gravity current. The dynamics of such current are often considered as belonging to hydraulic phenomena and are treated later in this book. In the case of Chesapeake Bay, the fresh surface outflow can be halted by upwelling-favorable winds blowing across the mouth. When these winds relax, the mass of released fresh water forms a buoyant current that exists the mouth, turns to the right, and flows southward along the coastline. The current remains trapped to the coastline by the effects of rotation and can have a striking blunt leading edge of nose that can be seen with the naked eye (see Figure 4.5.2).

This book explores the theories, idealized models, and laboratory experiments that have been developed in an attempt to understand the dynamics of these applications and to answer fundamental questions about their global significance. For example, does the horizontal circulation of deep water in a particular basin depend on whether the outflow is hydraulically controlled? Suppose that the world oceans were devoid of basins and deep passages. Would the production rates of various deep waters be unchanged? How would the rate of mixing between deep and shallow water masses be altered? The answers to these and other broad questions about the upstream and downstream influence of ocean and atmospheric choke points are not known, but the idealized models presented

herein give some clues. We hope that readers will be able to build on the basic material in order to develop new thinking and new approaches to long-standing problems.

*f) Further reading.*

There is an abundance of literature on the applications mentioned above. Specific citations will follow in discussions of deep ocean overflows (Sections 2.11 and 2.13), the California coastal marine layer (Sections 4.3 and 4.4), the Strait of Gibraltar (Sections 5.6 and 5.7) and others. For the reader seeking a more general discussion of the ocean deep circulation, Warren (1981) and the 2001 WOCE book: *Ocean Circulation and Climate: Observing and Modeling the Global Ocean* are good starting points. A brief history of the discovery of deep overflows can be found in Pratt and Lundberg (1990). An important landmark in this history is the Worthington and Wright (1971) atlas. Its maps of deep potential temperature surfaces suggesting penetration of dense intrusions into the deep North Atlantic inspired our Figure I6. The website “Sills of the Global Ocean” at [www.noc.soton.ac.uk/JRD/OCCAM/sills.html](http://www.noc.soton.ac.uk/JRD/OCCAM/sills.html) contains an extensive list of ocean sills that are potentially important in the distribution of deep water in the oceans. The oft-cited global conveyor belt is described by Broecker (1991) and on numerous websites.

## Figure Captions

I1 Hydraulically controlled, free-surface flow over a dam.

I2a Cloud cover near the N. California Coast on 05/17/02. (Image courtesy of Clive Dorman. )

I2b Velocity arrows and speed contours in the coastal marine layer From Pt. Arena to Bodega Bay, California. This is an earlier event than the one shown in I2a but there is a rough correspondence between the features. (Based on a figure from Winant et al. 1988.)

I2c A marine-layer gravity current flowing northwards along the California coastline. The arrows mark the leading edge and an eddy formed behind it.

I3. A three-layer version of the ocean thermohaline circulation. White bands indicate mean circulation within and above the main thermocline, gray represents deep circulation, and black represents bottom circulation.

I4 Maps of the oceans with smoothed versions of the 4000m and 5000m isobaths. Some well-known passages and the direction of flow through these passages are indicated. A bidirectional arrows indicate an exchange flow. a) The Atlantic ocean. The path of the section used in Figure I5 is shown as a dashed line. b) The Pacific Ocean. c) The Indian Ocean.

I5 A roughly north-south section through the western Atlantic showing selected deep potential density ( $\sigma_4$ ) surfaces, given in ( $\text{kg/m}^3$ ) minus 1000. The section track is shown in figure I6a. Water denser than 46.0 is considered Antarctic Bottom Water, and North Atlantic Deep Water has the density range  $45.5 < \sigma_4 < 45.9$ . The topographic spikes are isolated seamounts that do not impede the overall deep currents. This and Figure I6 were made by T. McKee and R. Curry using the Hydrobase data archive (<http://www.whoi.edu/science/PO/hydrobase>).

I6(a) The shaded area shows those portions of the Atlantic Ocean containing bottom water with potential temperature greater than  $1.8^\circ\text{C}$ . The edge of the shaded area is the intersection of the  $1.8^\circ\text{C}$  isothermal surface with the bottom. The contours overlain on the  $1.8^\circ\text{C}$  surface show its depth. The thin contours elsewhere show the 3000m isobath.

I6(b) Similar to Figure I6a, but for the  $1.0^\circ\text{C}$  potential temperature surface in the Pacific Ocean.

I6(c) Similar to Figure I6a, but for the  $1.0^\circ\text{C}$  potential temperature surface in the Indian Ocean.

I7 Longitudinal section of surface-referenced potential density ( $\sigma_\theta$ ), taken along the middle of the Denmark Strait. (From Figure 4 of Nikolopoulos et al. 2003).

I8 Potential density ( $\sigma_\theta$ ) across the Denmark Strait at (a) the sill and (b) approximately 50km downstream of the sill. The position of the section (E and L) are also indicated in Figure I7. (From Nikolopoulos et al. 2003.)

I9 Acoustic image with temperature profiles from Camerinal Sill in the Strait of Gibraltar. (Constructed using two figures from Armi and Farmer 1988).

I10 Map showing Jungfern and Grappler Passages. The deep throughflow is to the north. (from Fratantoni, et al. 1997).

I11 Cross-sections of potential temperature and along-strait velocity across the Grappler and Jungfern Passages (from Fratantoni et al. 1997).

I12 a) Normal velocity across the mouth of Chesapeake Bay. Positive values indicate outflow. b) Salinity distribution across the mouth of Chesapeake Bay. (From Levinson et al. 1998).

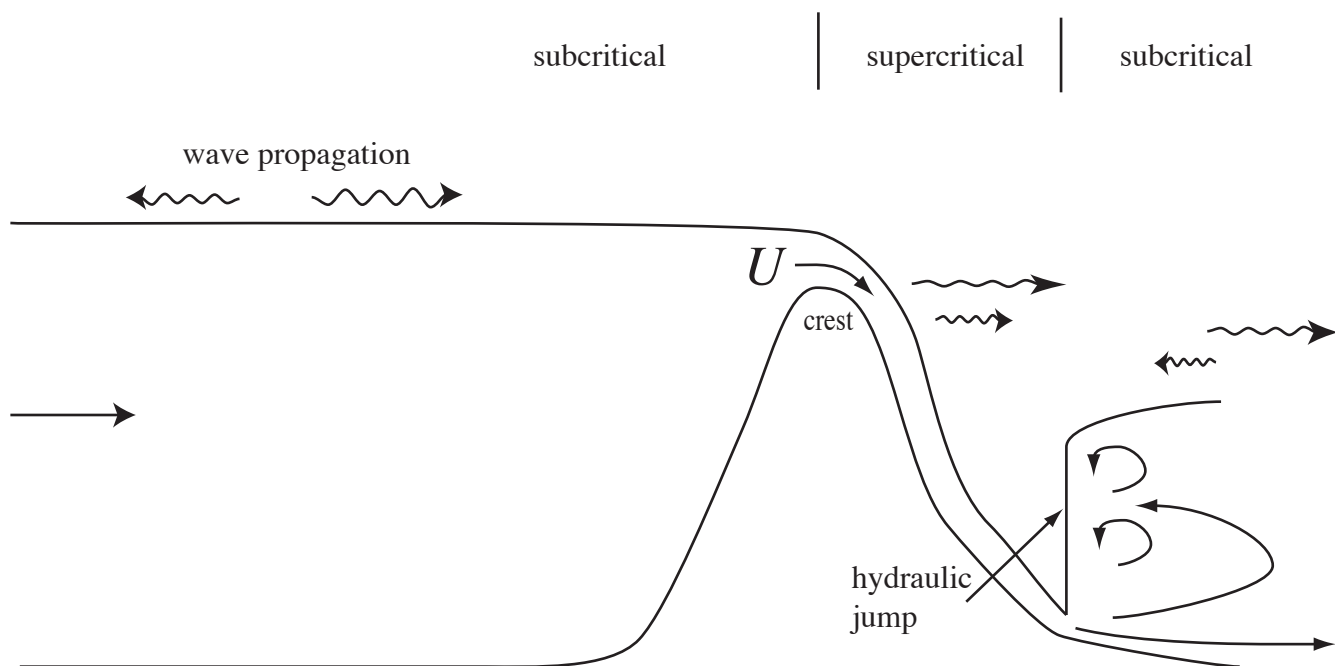


*Figure I1*

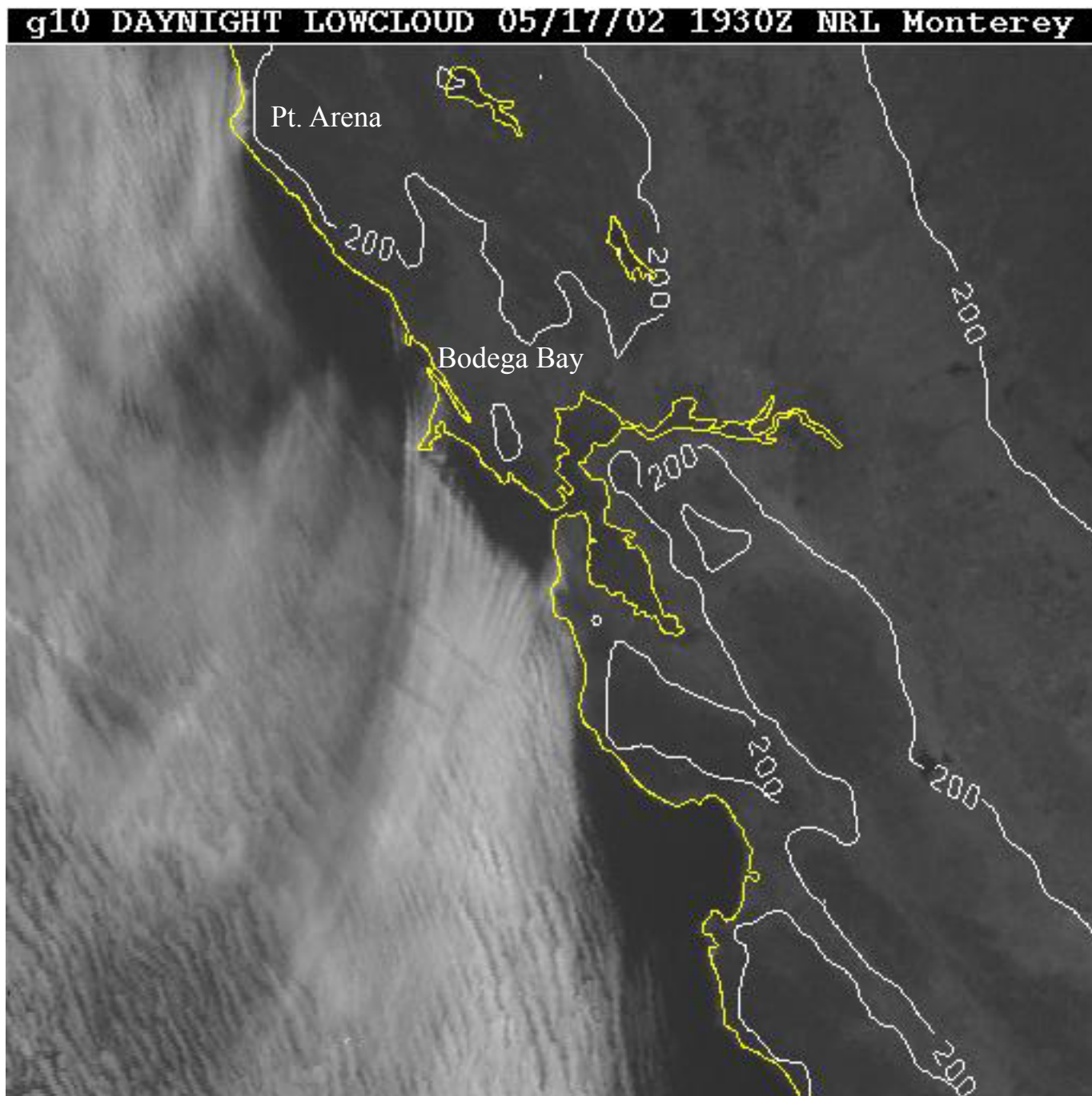


Figure I2a.

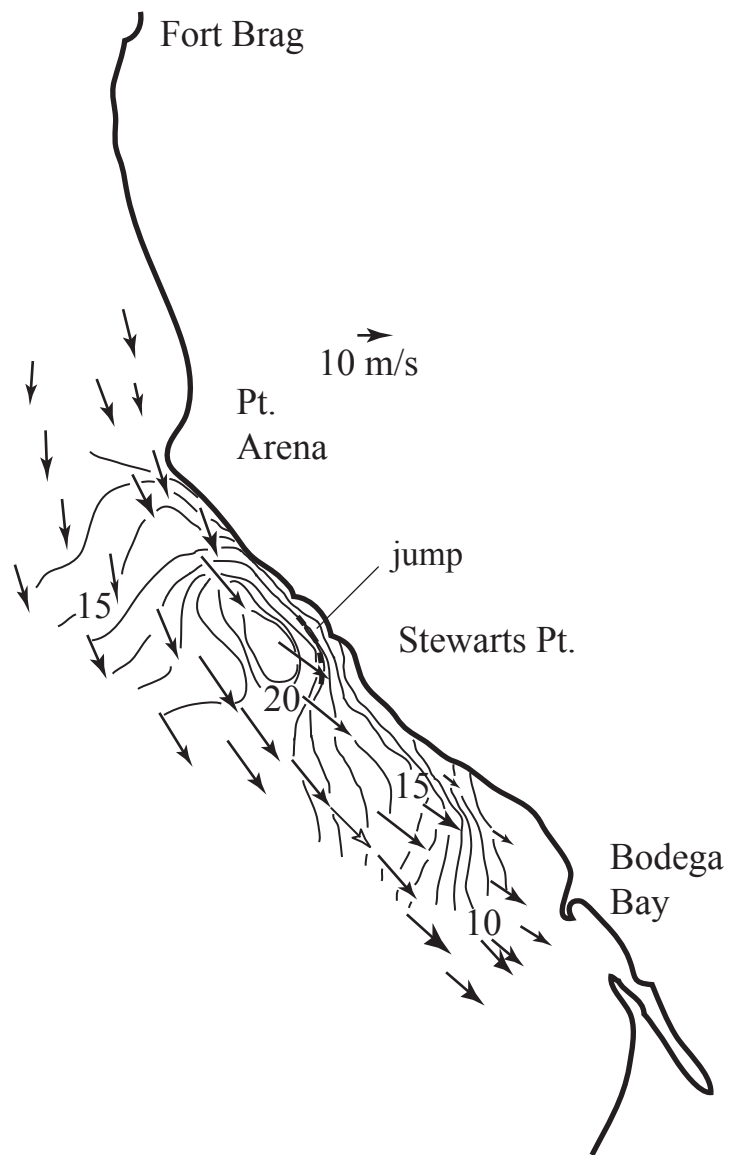


Figure 12b.

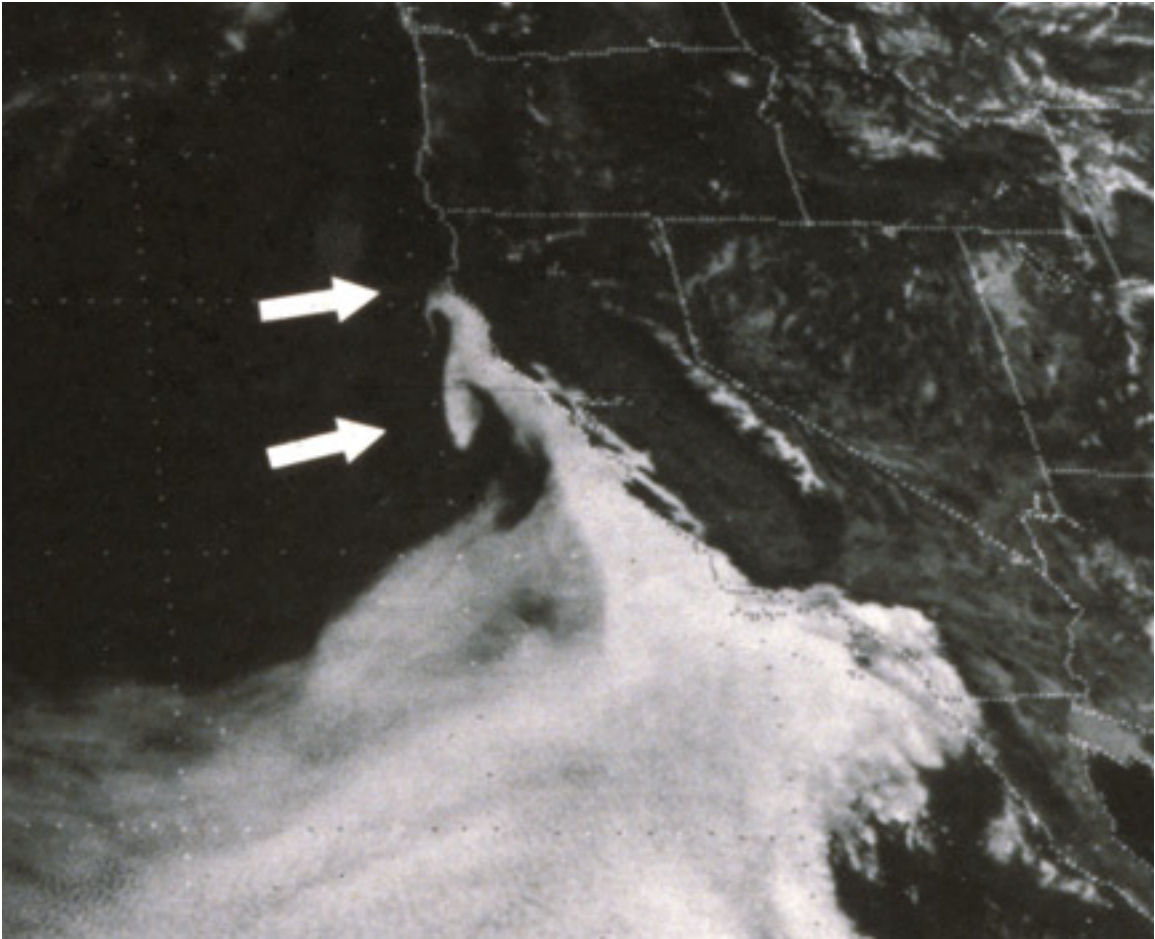


Figure I2c (cropped version)